

SOLUTION TO THE MULTI TERM BOLTZMANN EQUATION FOR PLASMA ASSISTED  
COMBUSTION

by

ANTRIKSH LUTHRA

Presented to the Faculty of the Graduate School of  
The University of Texas at Arlington in Partial Fulfillment  
of the Requirements  
for the Degree of

MASTER OF SCIENCE IN AEROSPACE ENGINEERING

THE UNIVERSITY OF TEXAS AT ARLINGTON

MAY 2010

Copyright © by Antriksh Luthra 2010

All Rights Reserved

*Dedicated to my grandfather, my parents and Dr. Luca Massa*

## ACKNOWLEDGEMENTS

I am truly grateful to my thesis advisor, Dr. Luca Massa, for his guidance and encouragement throughout this thesis. He has been a constant source of inspiration and has helped me improve my work on the regular basis.

I thank my graduate advisor, Dr. Kent Lawrence and Dr. Luca Madallena, Aerospace Engineering, for being a part of my thesis committee.

Finally, I am indebted my grandfather, my parents, my brother, Akash and my friend, Aruna for their continuous encouragement and support in all my endeavors.

May 14, 2010

## ABSTRACT

### SOLUTION TO THE MULTI TERM BOLTZMANN EQUATION FOR PLASMA ASSISTED COMBUSTION

Antriksh Luthra , M.S.

The University of Texas at Arlington, 2010

Plasma assisted ignition and combustion (PAIC) is a technology where plasma is generated by high voltage, nano second pulse duration and high repetitive rate pulses. The high reduced electric field during the pulse allows efficient electronic excitation and molecular dissociation, thereby generating a pool of chemically active radical species. This speeds up the reaction process needed to generate a high speed flame

A very high energy is liberated by collision of excited electrons with the neutral molecules of fuel in such a way that a minimal amount of energy go in momentum transfer. The majority of collision events are characterized by high kinetic energy so that the ionization takes place forming a pool of radicals which will in turn accelerate the chemical reactions.

The simulation of flame generated after the oxidation of radicals need their reaction rates and the reaction rates are directly proportional to the velocity distribution function of the excited electrons.

Multi term Boltzmann Equation is used in order to determine these electron velocity distribution functions at extreme reduced field conditions typical to hypersonic space flights.

## TABLE OF CONTENTS

ACKNOWLEDGEMENTS.....	iv
ABSTRACT.....	v
LIST OF FIGURES.....	ix
LIST OF TABLES.....	x
Chapter	Page
1. INTRODUCTION.....	1
1.1 High Speed Flame .....	2
2. THE BOLTZMANN TRANSPORT EQUATION.....	6
3. GOVERNING EQUATIONS AND SOLUTION APPROACH.....	9
3.1 The solution approach to Boundary Value problem .....	15
4. VALIDATION .....	21
5. METHANE ANALYSIS .....	26
5.1 Analytic Expressions.....	30
6. REACTION RATE COEFFICIENTS FOR METHANE.....	38
7. CONCLUSION.....	40
APPENDIX	
A. BOLTZMANN CODE .....	41
REFERENCES.....	49

BIOGRAPHICAL INFORMATION .....51

## LIST OF FIGURES

Table	Page
4.1 Velocity distribution function vs. Energy U .....	23
4.2 Velocity distribution function $f^k(U)$ , for $l = 8$ .....	25
5.1 Pressure versus altitude for a $M = 5$ flight .....	29
5.2 The cross section for methane breakdown into ions .....	31
5.3 Methane's vibrational modes at low electron energy .....	31
5.4 Distribution function At 40 eV, 100 Td and 100, 250,500,700 Td respectively .....	34
5.5 Velocity distribution function at 250 and 500 Td .....	35
5.6 Comparison of 2 term and 6 term approximation at 50 eV for methane at 100 and 500 Td respectively .....	36
5.7 Isotropic function expansion ( $k=0$ ) at various $E/N$ values .....	37
6.1 Reaction rate coefficient at different $E/N$ interval .....	39

## LIST OF TABLES

Table	Page
4.1 Comparison of mean electron energy $u_m$ and the drift velocity $w$ .....	24
5.1 Energy range and parameter of the Analytic Expressions for Methane (CH <sub>4</sub> ).....	32
5.2 Mean electron energy and drift velocity at 10 term approximation and 2 term approximation .....	33

## CHAPTER 1

### INTRODUCTION

Plasma assisted ignition and combustion (PAIC) is a new technology where plasma is generated by high voltage, nano second pulse duration and high repetitive rate pulses. The high reduced electric field (defined as the ratio of electric field to the molecule number density ( $E/N$ ) and expressed in Td units) during the pulse supports efficient electronic excitation and molecular dissociation, thereby generating a pool of chemically active radical species. The low duty cycle of the repetitive pulsed discharge improves the discharge stability and helps creating a diffuse, uniform and volume filling non equilibrium plasma.

Its range of application covers hypersonic space flights, gas turbines for terrestrial power generator and flue gas treatment.

At a very high Mach number, typical to hypersonic space flights, supersonic mixing layers feature a low linear growth rate. The supported low mixing implies that reaction must proceed at low equivalence ratios. Plasma assisted combustion enhances the combustion performance in low equivalence ratios.

Plasma is an ionized gas made of electrons and positive ions. Generally the number densities of opposite charged particles have the same magnitude, so weakly ionized plasma is in quasi neutral state. During ionization, electrons are the first in receiving the energy from the

electric field because of their high mobility and low mass and this energy. Energy is then transferred to by the electrons to the neutral particles through various elastic and inelastic collisional processes like dissociation, attachment etc.

The rate at which ionization processes take place depends upon the number of electron having enough energy to participate in an inelastic collision event. Statistically, electron energy can be described by the electron energy distribution function. It is the probability density  $f(U)$  for an electron to have energy  $U$ .

The determination of this density function and finding out the reaction rate coefficient is goal of this research. The chemical rate of production of charged particles will be later used to find adiabatic flame speed and induction times under plasma conditions.

### 1.1 High Speed Propulsion

The development of hypersonic flight vehicles requires efficient energy conversion. Due to the large loss in total pressure occurring in the supersonic to subsonic transition process, hypersonic thrust generators utilize supersonic combustors, a configuration known as scramjet. Supersonic mixing-layers are characterized by a low mixing rate evaluated with respect to the convective time scale, so that reaction must proceed at low equivalence ratios, i.e., fuel lean combustion. Therefore, in order transfer energy efficiently to the working fluid, the chemical time in fuel lean conditions has to be large compared to the convective time. This consideration limits the use of hydrocarbon fuels for supersonic combustion, because in air-fuel mixtures the chemical time decreases quickly away from the stoichiometric condition. In the scenario of

supersonic air-breathing propulsion hydrocarbon fuels are less competitive than hydrogen. Nonetheless, hydrogen fuel has many drawbacks, including very low energy density by volume and various safety concerns, [1]. The new version of the NASA X-43 hypersonic aircraft is designed to use hydrocarbon fuel as energy generator. Plasma-assisted ignition and combustion (PAIC) is a new technology that uses non-thermal plasma to enhance combustion performance at low equivalence ratios, [2, 3].

The range of application of plasma combustion goes beyond hypersonic flight. Lower equivalence ratios in a combustion process imply a lower adiabatic flame temperature which leads to a reduction in the rate of entropy production in the combustor (proportional to the difference between flame temperature and maximum cycle temperature) and to a decrease in the formation of  $\text{NO}_x$  products. Thus, this technology appeals to ground energy generation as well.

The fundamental question in assessing performance of plasma combustion is to quantify the advantage of the non-thermal energy transfer when compared to the thermal analog. Energy exchange through fast electron collisions excite internal and electronic energy states moving the reagents away from thermal (Boltzmann) equilibrium. The combustion field supported by plasma discharge presents two main regions of heat release, the “cool flame.”([5]), i.e., plasma activated initial oxidation, and the final flame, thermally activated heat release, which at nominal flow rates occurs outside the discharge area. Exothermic chemical reactions at both flame fronts are characterized by large activation barriers, and therefore are selective with respect to the reagents state. Understanding energy consumption and tunneling of internal

modes into bond breaking motion is the main path to a better design of plasma enhancing systems.

The rationale for the previous statement is the link between reduced electric field and electron energy, and between electron energy and internal mode excitation: low energy collisions result in a large momentum transfer, mid-range collision in vibrational modes, and high energy in ionization and dissociation. Different types of plasma discharges ( e.g., nano-pulsed, radio-frequency, microwave-frequency) were shown to produce different levels of laminar flame speed enhancement, [6], suggesting that an increased electron energy leads to a more efficient chemical activation. Furthermore, the relationship between reduced field ( $\propto \frac{1}{p}$ ) and electron energy makes the excitation processes pressure dependent. Thus a study of plasma/combustion chemistry is necessary to understand the response of the combustor to changes in altitude.

The chemistry model must take into account the different forms of internal molecular energy, and consider a vast range of chemical processes including: the electron impact collision processes in the discharge region, the selectivity of the reactions to the internal state of the molecules, and the ion and radical chemistry known to be pressure sensitive. The detailed chemistry model is likely to contain several hundred species and thousands reactions.

Our overall goal is to analyze the sensitivity of the rate of reactions and how the expansion order affects the flame speed. The resultant rates will be used in flame speed calculations.

To determine the reaction rates we make use of the Boltzmann Equation (will be discussed in detail in later section).

For the solution of the Boltzmann equation related to steady-state plasma conditions the most easily achievable solution is through BOLSIG, a 2 term approximation Boltzmann equation solver, but the solution is inaccurate at very high reduced electric field. Efforts have been undertaken to develop techniques that make a solution of the kinetic problem in higher order accuracy possible.

The techniques related to steady-state plasmas are based on quite different procedures such as (i) an higher order expansion in Legendre polynomials of the velocity distribution in the relevant kinetic equation, and the numerical solution of the resultant differential equation system by a GALERKIN approach [18] or by a complicated direct integration of the system [19,10] (ii) the velocity moment method [21] including a complex approximation of the velocity distribution and (iii) the direct numerical integration of the kinetic equation avoiding a further expansion of the velocity distribution [20]. All these techniques are more or less sophisticated, and of large complexity.

## CHAPTER 2

### THE BOLTZMANN TRANSPORT EQUATION

The Boltzmann equation, also often known as the Boltzmann transport equation, devised by Ludwig Boltzmann, describes the statistical distribution of one particle in a fluid. The Boltzmann equation is used to study how a fluid transports physical quantities such as heat and charge, and thus to derive transport properties such as electrical conductivity, Hall conductivity, viscosity, and thermal conductivity.

The Boltzmann equation is an equation for the time  $t$  evolution of the distribution (properly a density) function  $f(x, p, t)$  in one-particle phase space, where  $x$  and  $p$  are position and momentum, respectively.

The macroscopic properties of the electrons can be obtained by solving the relevant electron Boltzmann equation as to determine the velocity distribution function of the electrons and performing the corresponding averages over the velocity distribution. It is well known that the velocity distribution function of the electrons in a weakly ionized plasma represents a link between the microscopic processes acting upon the electrons in the plasma (characterized e.g. by the atomic data of the electron collision processes and the electric field) and the various macroscopic properties of the electrons (as mean energy, drift velocity or mean collision frequencies).

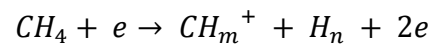
However, some of the atomic data of the relevant electron collision processes are often not known or their values are very uncertain. To fit some of the uncertain atomic data of the collision processes, a repeated determination of the velocity distribution and of corresponding macroscopic properties of the electrons has to be performed by solving the electron kinetic equation.

In few special cases i.e. that of the electrons in steady-state plasmas and of the swarm electrons subjected to constant electric fields finally time- and space-independent kinetic equations are obtained and solutions to these have been sought to higher order accuracy.

The technique used in present research is based upon multi-term expansions of the electron velocity distribution in Legendre polynomials. The resultant partial differential equation systems for the expansion coefficients is solved as initial-boundary value problems by using appropriately adapted finite differences approaches. An important point in this respect has been the choice of the proper boundary conditions for the expansion coefficients of the velocity distribution. The boundary conditions used here have been deduced from a former detailed asymptotic analysis [10,20] of the corresponding system of equations relevant to time- and space-independent plasmas.

The data for the production of neutral hydrocarbon fragments are coupled with those representing production of hydrogen and hydrocarbon cat ions to produce rate for the elementary processes,





,where  $m + n = 4$ ,  $m = 1, \dots, 4$ . Vibrational cross section data for the four normal modes (multiplied by the respective multiplicities) of the methane molecule are taken from Nishimura and Gianturco, [7].

## CHAPTER 3

### GOVERNING EQUATIONS AND SOLUTION APPROACH

The time independent Boltzmann Equation governing the microscopic properties of the electron in steady state Plasmas is given as follows:-

$$-\left(\frac{e_0}{m_e}\right)E \cdot \nabla_{\mathbf{t}}F = C_{\text{el}}(F) + \sum_m C_{\text{in}}(F)$$

$$\int F(v)dv = 1 \tag{1}$$

Where  $F(v)$  is the electron velocity distribution function,  $e_0$  is the electron charge,  $m_e$  is the electron mass.

$E$ , Electric field in the steady state plasma remains constant. The gas particles are assumed to be at rest and in the ground state and to have the mass  $M$  and the density  $N$ .

The impact of elastic and first kind inelastic collisions of the electrons with the gas particles is taken care by the right-hand side of (1) in terms of the collision integrals  $C_{\text{el}}$  and  $C_{\text{in},m}$ .

The index  $m$  denotes the  $m^{\text{th}}$  inelastic collision process considered.

An additional inclusion of second kind inelastic collisions with excited gas particles in the kinetic equation (1) and its solution approach is immediately possible. However, for simplicity of the further representation, first kind inelastic collisions only are considered.

Since steady-state plasmas are under consideration, for each inelastic collision the number of electron particles is conserved. Thus, the electron density assumes a constant value and the velocity distribution can be normalized per one electron. Such a normalization has been already adopted and expressed in (1) by the normalization condition.

Furthermore, the constant electric field is supposed to be parallel to the z-axis of the chosen coordinate system, i.e.  $E = Ee_z$  with  $e_z$  being the unit vector in the z-direction. Then, with the magnitude  $v$  of the velocity  $\mathbf{v}$  given by  $v = (v_x^2 + v_y^2 + v_z^2)^{1/2}$ , the velocity distribution function  $F(\mathbf{v})$  is reduced dependence  $F(v, v_z/v)$  and can be expanded with respect to  $v_z/v$  into Legendre polynomials  $P_n(v_z/v)$ . In l-term approximation this expansion reads

$$F\left(v, \frac{v_z}{v}\right) = \sum_{k=0}^{l-1} f^k(v) P_k(v_z/v) \quad (2)$$

When substituting this expansion into (1) and replacing the velocity magnitude  $v$  by the kinetic energy  $U = m_e v^2/2$ , the hierarchy of ordinary differential equations,

$$\begin{aligned} & -\left(\frac{e_0 E}{3N}\right) \left( \frac{d}{dU} (U f^{(1)}(U)) - \frac{d}{dU} \left[ \left( \frac{U^2 2m_e}{M} \right) (Q_{el}^{(0)}(U) - Q_{el}^{(1)}(U)) f^0(U) \right] \right) \\ & + \sum_m U Q_{in,m}^0(U) \times f^0(U) - \sum_m (U + U_{in,m}) Q_{in,m}^0(U + U_{in,m}) f^{(0)}(U + U_{in,m}) \\ & = 0 \end{aligned}$$

$$\begin{aligned}
& -\frac{k}{2k-1} e_0 \left( \frac{E}{N} \right) \left[ U \frac{d}{dU} f^{(k-1)}(U) - \frac{k-1}{2} \times f^{(k-1)}(U) \right] \\
& -\frac{(k+1)}{2k+3} e_0 \left( \frac{E}{N} \right) \left[ U \frac{d}{dU} f^{k+1}(U) + \frac{k+2}{2} f^{k+1}(U) \right] \\
& + \left( Q_{el}^{(0)}(U) - Q_{el}^{(k)}(U) + \sum_m Q_{in,m}^{(0)}(U) \right) U \times f^{(k)}(U) \\
& - \sum_m (U + U_{in,m}) Q_{in,m}^{(k)}(U + U_{in,m}) f^k(U + U_{in,m}) = 0
\end{aligned}$$

$$\begin{aligned}
& \frac{l-1}{2l-3} e_0 \left( \frac{E}{N} \right) \left[ U \frac{d}{dU} (f^{l-2}(U)) - \frac{l-2}{2} f^{l-2}(U) \right] \\
& + \left( Q_{el}^{(0)}(U) - Q_{el}^{(l-2)}(U) + \sum_m Q_{in,m}^{(0)}(U) \right) U f^{(l-1)}(U) \\
& - \sum_m (U + U_{in,m}) Q_{in,m}^{(l-1)}(U + U_{in,m}) f^{(l-1)}(U + U_{in,m}) \\
& = 0
\end{aligned} \tag{3}$$

for the transformed expansion coefficients

$$f^{(k)}(U) = 2\pi(2/m_e)^{3/2} f^{(k)}(v(U)), \quad k = 0, 1, 2 \dots \dots l-1,$$

with the corresponding normalization condition

$$\int_0^\infty U^{\frac{1}{2}} f^{(0)}(U) dU = 1 \tag{4}$$

for the lowest transformed expansion coefficient  $f^{(0)}(U)$  is obtained [11,12].

On deriving hierarchy (3), because of the smallness of the electron mass  $m_e$  compared with the gas particle mass  $M$  each collision integral has been additionally expanded with respect to the mass ratio  $m_e/M$ , and this expansion has been truncated after the leading term.

Also the term with the shifted energy arguments  $U + U_{in,m}$  are due to the electrons with the energy  $U + U_{in,m}$  which have undergone inelastic collisions of the  $m_{th}$  process and are backscattered to the energy  $U$  because of their energy loss  $U_{in,m}$  in this process.

There is sequences of generalized total collision cross sections, due to the expansion of (1) and thus of the collision integrals involved when substituting (2),

$$Q_{el}^{(k)}(U) = \int \sigma_{el}(U, \cos\theta) P_k(\cos\theta) \sin\theta d\theta d\epsilon$$

$$Q_{in,m}^{(k)}(U) = \int \sigma_{in,m}(U, \cos\theta) P_k(\cos\theta) \sin\theta d\theta d\epsilon, \quad (5)$$

with  $k = 0 \dots L - 1$  occur in the hierarchy equations (3).

These cross sections are obtained by integrating the respective differential cross section  $\sigma_{el}(U, \cos\theta)$  and  $\sigma_{in,m}(U, \cos\theta)$  times the Legendre polynomials  $P_k(\cos\theta)$  over the solid scattering angle  $\sin\theta d\theta d\epsilon$ .

The impact of the anisotropic scattering in elastic collisions and the various inelastic collision processes in the hierarchy equations (3) is described by sequences (5).

In case of isotropic scattering all generalized cross sections (5) for  $k = 0 \dots L - 1$  become zero and only the respective total cross section  $Q_{el}^{(0)}(U)$  and  $Q_{in,m}^{(0)}(U)$  of each collision process remains in hierarchy (3).

The difference  $Q_{el}^{(0)}(U) - Q_{el}^{(1)}(U)$ , observable in the first two equations of (3), represents momentum transfer cross section  $Q_a(U)$  of elastic collisions.

Treating the system of equations (3) directly as a boundary-value problem is the basic idea of the solution approach presented below the boundary value problem is integrated in the energy range  $0 < U < U_\infty$ , where  $U_\infty$  denotes an appropriate upper energy limit.

To develop such an approach adequate boundary conditions for all coefficients  $f^{(k)}(U)$  involved in the expansion (2) are needed. As mentioned above, specific information on the solution manifold of system (3) has already been obtained in the past [12] while performing an asymptotic analysis of this ordinary differential equation system for low and high kinetic energies. It was found that the equation system is weakly singular at low and strongly singular at high kinetic energies. As a consequence the general solution of e.g. each even-order multi-term solution of the hierarchy (3) contains an equal number, namely half the even order, of singular and nonsingular contributions to the general solution.

This property holds at both, i.e. at low and high kinetic energies. The physically relevant solution has to be sought within the nonsingular part of the general solution.

To isolate by separate conditions at high as well as at low kinetic energies the nonsingular part of the general solution and to find in this way the physically relevant solution of hierarchy (3), a sophisticated technique has been developed already [9].

These insights into the solution structure of the system (3) have been the basis for the multi-term treatment of the electron kinetics of the respective time- and space-dependent plasmas [13a, 13b].

Appropriate boundary conditions for the expansion coefficients have been formulated in these more complex cases when treating the kinetic equation in multi-term approximation as initial-boundary value problems.

In the limit of time- and space-independent, i.e. steady-state plasmas, the corresponding boundary conditions used in both cases assume the same representation and read [13a]

$$\begin{aligned}
 f^{(k)}(U = 0) &= 0, & k &= 1,3,5 \dots \\
 f^{(k)}(U = U_\infty = 0), & & k &= 0,2,4 \dots \\
 f^{(k)}(U > U_\infty) &= 0 & k &= 0,1,2,3 \dots
 \end{aligned} \tag{6}$$

Significantly, as in time- and space-dependent plasmas the boundary conditions (6) enforce a suppression to the singular contributions of the relevant solution of system (3) at low as well as at high kinetic energies.

The first two lines of (6) are the real boundary conditions of the pure ordinary differential equation part of system (3). The last line of (6) represents the natural demand that all contributions to the velocity distribution, i.e. all coefficients of expansion (2), become negligibly small for energies  $U$  larger than  $U_\infty$ . As a consequence all backscattering terms in system (3), caused by inelastic collisions and characterized by the shifted energies  $U + U_{in,m}$  will be neglected if these shifted energies become larger than the upper limit  $U_\infty$  of the relevant energy range. The governing equations analyzed in the present research are similar to what is used in reference [8].

### 3.1 The Solution Approach to Boundary Value Problem

System (3) for the  $l$  expansion coefficients,

$f^{(0)}(U) \dots f^{(l-1)}(U)$  is solved as a boundary value problem using a finite differences approach. To derive an appropriate finite differences equation system for the expansion coefficients from system (3). Its discretization at all centered points:-

$$U_{i+\frac{1}{2}} = U_i + du/2$$

of the equidistant energy mesh  $U_i$ .  $1 < i \leq n_\infty + 1$ , with the energy boundaries

$$U_1 = 0 \text{ and } U_{n_\infty+1} = U_\infty$$

and the step size  $\Delta U$  is performed. When henceforth abbreviating  $f^{(k)}(U)$  by  $f_i^{(k)}$ , the discretized function values  $f_{i+1/2}^{(k)}$  and their derivatives at  $U_{i+1/2}$  are approximated by the second-order-correct representation [13a].

$$f_{i+\frac{1}{2}}^{(k)} = \frac{1}{2}(f_i^k + f_{i+1}^k)$$

$$\left(\frac{d}{dU}(f_i^k(U))\right)_{i+\frac{1}{2}} = \frac{1}{\Delta U}(f_{i+1}^k - f_i^k) \quad (10)$$

Each function value belonging to a shifted energy argument is represented on the equidistant mesh by means of a parabolic interpolation using the three most neighboring discrete values of the same function to the shifted energy points,  $U_{i+\frac{1}{2}} + U_{in,m}$ . Such an interpolation has the representation [13a].

$$f^k\left(U_{i+\frac{1}{2}} + U_{in,m}\right) = \left(\frac{1}{2}\right)\alpha_m^{-3}\alpha_m^{-1}f_{n_m+i}^k - \alpha_m^1\alpha_m^{-3}f_{i+n_m+1}^k + \left(\frac{1}{2}\right)\alpha_m^1\alpha_m^{-1}f_{i+n_m+2}^k \quad (11)$$

$$n_m = \text{int}(U_{in,m}/\Delta U),$$

$$\alpha_m^j = (U_{in,m}/\Delta U) - n_m + j/2$$

where  $j = 1, -1, -3$

Where,  $\text{int}(x)$  is the integer part of  $x$ .

The substitution of (10) and (11) into the equation system (3) leads finally to the discrete equation system:-

$$r_i^1 f_i^1 + s f_{i+1}^1 + e f_i^0 + g_i f_{i+1}^0 = d_i^0$$

$$r_i^{k+1} f_i^{k+1} + s_i^{k+1} f_i^{k+1} + p_i^k f_i^k + p_i^k f_{i+1}^k + v_i^{k+1} f_i^{k-1} + w_i^{k+1} f_{i+1}^{k-1} = d_i^k, \quad 1 \leq k \leq l-2.$$

$$p_i^{l-1} f_i^{l-1} + p_i^{l-1} f_i^{l-1} + v_i^l f_i^{l-2} + w_i^l f_{i+1}^{l-2} = d_i^{l-1} \quad (12)$$

For,  $i = l \dots n_\infty$  With the coefficients

$$e_i = -D_i + \frac{F_i \Delta U}{2}, \quad g_i = D_i + \frac{F_i \Delta U}{2}, \quad p_i^k = \frac{H_i^k \Delta U}{2}$$

$$r_i^k = \frac{k}{2k+1} e_0 \left( \frac{E}{N} \right) \left( U_{i+\frac{1}{2}} - \frac{k+1}{2} \left( \frac{\Delta U}{2} \right) \right)$$

$$s_i^k = -\frac{k}{2k+1} e_0 \left( \frac{E}{N} \right) \left( U_{i+\frac{1}{2}} + \frac{k+1}{2} \left( \frac{\Delta U}{2} \right) \right)$$

$$v_i^{k+1} = \frac{k}{2k-1} e_0 \left( \frac{E}{N} \right) \left( U_{i+\frac{1}{2}} - \frac{k-1}{2} \left( \frac{\Delta U}{2} \right) \right)$$

$$w_i^k = \frac{k}{2k-1} e_0 \left( \frac{E}{N} \right) \left( -U_{i+\frac{1}{2}} - \frac{k-1}{2} \left( \frac{\Delta U}{2} \right) \right)$$

$$k = 1, \dots, l-1 \quad (13)$$

Some more coefficient involved:

$$D_i = -U_{i+\frac{1}{2}}^2 2 \left( \frac{m_e}{M} \right) Q_d \left( U_{i+\frac{1}{2}} \right),$$

$$F_i = -U_{i+\frac{1}{2}}^2 2 \left( \frac{m_e}{M} \right) \left( 2Q_d \left( U_{i+\frac{1}{2}} \right) + U_{i+\frac{1}{2}} \times \frac{Q_d(U_{i+1}) - Q_d(U_i)}{\Delta U} \right) + U_{i+\frac{1}{2}} \sum_m Q_{in,m}^{(0)} \left( U_{i+1/2} \right)$$

$$H_i^k = U_{i+1/2} [(Q_{el}^0(U_{i+1/2}) - Q_{el}^k(U_{i+1/2})) + \sum_m Q_{in,m}^0(U_{i+1/2})] \quad (14)$$

The terms on the right-hand side of the discrete equation system (12) reads,

$$d_i^k = - \sum_m \Delta U \times I_{i,m}^k \left( \left(\frac{1}{2}\right) \alpha_m^{-3} \alpha_m^{-1} f_{n_m+i}^k - \alpha_m^1 \alpha_m^{-3} f_{i+n_m+1}^k + \left(\frac{1}{2}\right) \alpha_m^1 \alpha_m^{-1} f_{i+n_m+2}^k \right),$$

$$0 \leq k \leq l - 1$$

$$\text{With, } I_{i,m}^k = - \left( U_{i+1/2} + U_{in,m} \right) Q_{in,m}^k (U_{i+1/2} + U_{in,m}) \quad (15)$$

The discrete form of the boundary conditions (6) is,

$$f_{n_\infty+1}^k = 0 \text{ for } k = 0,2,4 \dots \dots$$

$$f_1^k = 0 \text{ for } k = 1,3,5 \dots \dots$$

$$f_i^k = 0 \text{ for } k = 0,1,2,3,4 \dots \dots \text{ and } i > n_\infty + 1 \quad (16)$$

A formal consideration of the discrete equation system (12) and the discrete boundary conditions (16) shows that the number  $I \times (n_\infty + 1)$  of equations equals the number of discrete function values  $f_i^{(k)}$  on the mesh.

However, the system consists only of homogeneous and linear equations. In order to avoid that the trivial solution of the system is finally obtained, a slight modification of the system is needed. It has been found that this modification can be performed in a very appropriate way if

the discretized version of the normalization condition (4) is added to the system (12) and the very first of the equations (12), i.e. the equation,  $r_1 f_1^{(1)} + s_1 f_2^{(1)} + e_1 f_1^{(0)} + g_1 f_2^{(0)} = d_1^0$  is cancelled as to keep the total number of equations the same as the number of discrete function values.

The discretization of (4) has been performed by using SIMPSON's rule with respect to the interval  $0 \leq U \leq U_\infty$  assuming that an even number  $n_\infty$  of energy intervals is henceforth considered. As to keep the numerical error contribution in the neighborhood of  $U = 0$  small, the rule for the first double interval  $0 < U < 2\Delta U$  has been improved by applying the substitution  $x = U^{3/2}$  and a succeeding replacement by parabolic interpolation of that function value which does no longer fit into the energy mesh. The discrete version of the normalization condition derived in this way [14] finally reads,

$$h_1 f_1^0 + h_2 f_2^0 + \dots + h_{n_\infty} f_{n_\infty}^0 + h_{n_\infty+1} f_{n_\infty+1}^0 = 3/\Delta U$$

With coefficients,

$$\lambda = 2/4^{1/3}$$

$$h_1 = \left(\frac{2}{3}\right) (2\Delta U)^{\frac{1}{2}} (1 + 2(\lambda - 1)(\lambda - 2))$$

$$h_2 = -8/3(2\Delta)^{\frac{1}{2}} \lambda (\lambda - 2)$$

$$h_3 = \left(\frac{2}{3}\right) (2\Delta U)^{\frac{1}{2}} (1 + 2\lambda(\lambda - 1)(\lambda - 2))$$

$$h_{2i} = 4 \times U_{2i}^{1/2}$$

$$h_{2i+1} = 2U_{2i+1}^{1/2}, i = 2, 3 \dots, (n_{\infty} - 2)/2$$

$$h_{n_{\infty}} = 4U_{n_{\infty}}^{1/2}$$

$$h_{n_{\infty}+1} = U_{n_{\infty}}^{1/2} \tag{18}$$

Unlike the method used in reference [8] to solve this boundary value problem, which make use of formation of a triangular band algorithm to systematically arrange the matrix coefficient with respect to distribution function at various discretized points, we made use of sparse matrix system using matlab.

I have written and validated a easy to use Matlab program for the solution of electron energy distribution function in steady state plasmas and the integration of source terms. The Program which repeated in appendix 1 provides input for combustion codes in term of kinetic rate constants against mean electron energy.

## CHAPTER 4

### VALIDATION

#### Model Gas

A model gas, as considered in the former paper [11] and reference [8] is used to match our results and to illustrate multi-term solution technique.

The particles of the model gas are characterized by a mass

- M of 4 amu,
- Energy-independent total cross section  $Q_{el}^{(0)}(U) = 6 \cdot 10^{-16} \text{ cm}^2$  for elastic collisions and by a single excitation process with the energy loss  $U_{in.1} = 1 \text{ eV}$ .
- The total cross section  $Q_{in,1}^0(U)$  of the latter is supposed to increase linearly from 0 at  $U = U_{in.1}$  to  $6 \cdot 10^{-16} \text{ cm}^2$  at  $U = U_{in.1} + 0.2 \text{ eV}$  and to remain then constant for higher energies U.

For elastic collisions, the differential cross section is supposed to have a form:

$$\sigma_{el}(U, x) = Q_{el}^0(U) \times \left(\frac{1}{2\pi}\right) \times R_{el}(x), \quad x \equiv \cos\theta$$

$$R_{el}(x) = \frac{1}{a} \times \exp\left(-\frac{(x-x_{el}^M)^2}{s_{el}^2}\right)$$

$$a = \int_{-1}^1 \exp\left(-\frac{(x-x_{el}^M)^2}{s_{el}^2}\right) dx \quad (18)$$

i.e., a Gaussian scattering profile  $R_{el}(x)$  with the normalization,  $\int_{-1}^1 R_{el}(x)dx$  and with the centre  $x_{el}^M$  and the width  $s_{el}$  is used for all electron energies. The isotropic scattering is included in (18) by the limit,  $s_{el} \rightarrow \infty$ , i.e. by  $R_{el}(x) = 0.5$ . The differential cross section  $\sigma_{elin,1}(U, x)$  of the excitation process is described by the same representation (18), however, with the centre  $x_{in,1}^M$  and the width  $s_{in,1}$ .

With respect to the elastic collisions as well as to the single inelastic collision process, two scattering conditions, namely isotropic scattering with  $R_{\tau}(x) = 0.5$ ,  $\tau = el$  and in,1 and pronouncedly forward scattering with the centre  $x_{\tau}^M = l$  and the width  $s_{\tau} = 0.5$ , are considered. These two scattering conditions are henceforth denoted by iso-el and aniso-el for elastic collisions and by iso-in and aniso-in for the single excitation process.

The test conditions are :

- reduced electric field  $E/p_0 = 17.7 \text{ V cm}^{-1} \text{ Torr}^{-1}$ .
- Here  $p_0$ , introduced according to  $p_0 = N/n_g$  with  $n_g = 3.54 \cdot 10^{16} \text{ cm}^{-3} \text{ Torr}^{-1}$ , denotes the gas pressure at  $0^\circ\text{C}$ . Particularly, when going from isotropic scattering to distinctly anisotropic scattering in elastic collisions, a large change of both distribution parts results.

The ionization of the molecules occurs due to distribution of energies. Figure 4.1 shows the distribution function with respect to the electron energy, it can be observed that the distribution function equals to zero for higher energy values in the case of model gas.

Electron energy distribution for the model gas

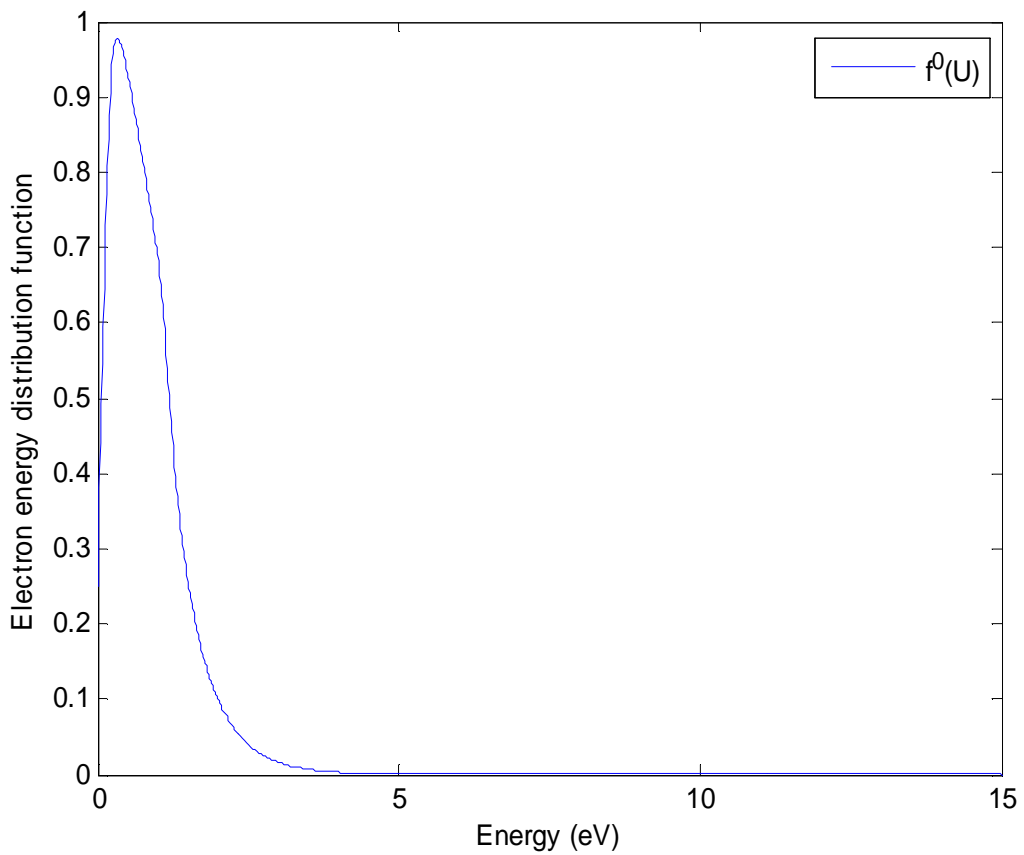


Fig 4.1: Electron energy distribution function vs. Energy U

Also, the mean electron energy and the drift velocity is given as follows:

$$u_m = \int_0^\infty U^{\frac{3}{2}} f^0(U) dU$$

$$w = -\frac{1}{3} \left( \frac{2}{m_e} \right) \int_0^\infty U f^1(U) dU$$

In the following table 4.1, both mean electron energy and drift velocity are tabulated under the column 'Present'.

Table 4.1: Comparison of mean electron energy  $u_m$  and the drift velocity  $w$

$l$	$u_m$ [eV]		$w$ [ $10^7$ cm s $^{-1}$ ]	
	Reference 1	Present	Reference 1	Present
2	1.121	1.1217	3.881	3.8838
4	1.052	1.0528	3.481	3.4836
6	1.046	1.0470	3.483	3.4851
8	1.046	1.0471	3.482	3.4847

There is an excellent agreement with the solution obtained and solution provided in reference

[8] for every  $L$  and  $\frac{E}{p_0} = 17.7$  V cm $^{-1}$ Torr $^{-1}$ .

The agreement of the result obtained validates the accuracy of the method used to obtain the multi term solution.

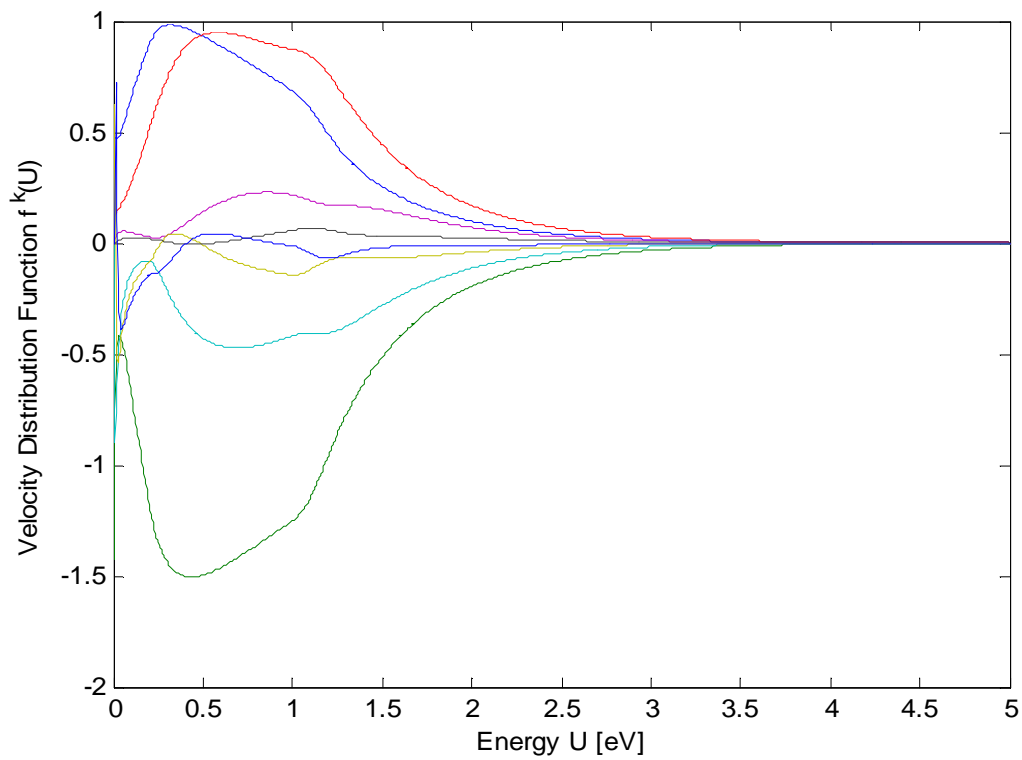


Fig 4.2: Distribution functions  $f^k(U)$ , for  $l = 8$

Velocity distribution under 8 term approximation for higher and lower term together is shown in figure 4.2.

## CHAPTER 5

### METHANE ANALYSIS

After successfully applying the Boltzmann Transport equation to the model gas, I switch my attention to gases for practical combustions applications.

The analysis considers the combustion of alkanes in air. Methane will be the primary fuel choice due to the simplicity of the molecule. Experiments on plasma enhanced combustion of methane are described in [15]; the molecule behaves similarly to higher atomic mass alkanes. In combustion computational analysis the kinetic rates appear in the energy and species concentration of all relevant chemical species plus the electrons. Therefore the rates described in this section are of critical importance to the analysis of Plasma assisted combustion.

Methane gas has considerably large inelastic cross sections which are comparable to or even greater than momentum transfer cross section at low electron energies (0.3 eV) and high electron energies ( $\geq 20$  eV). (see, for example, Ohmori 1986). At such conditions, techniques such as 2-term approximation simulations have not given satisfactory results.

As discussed earlier that hypersonic space flights needs efficient energy conversion and large amount of energy is lost in supersonic and subsonic transition. As the Mach no increases, the entropy change across the shock waves also increases which results in a strong entropy gradient and vertical flow which mixes the boundary layers.

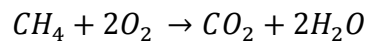
These supersonic mixing of layers are characterized by low mixing rate (evaluated with respect to the convective time scale). In order to maintain that, reactions must proceed at a low equivalent ratios i.e. fuel lean combustion. The motive of low mixed ratio is also to achieve lower adiabatic flame temperature leading to reduction of rate entropy production and  $NO_x$  production.

The equivalence ratio for 1 mole of methane and 1 mole of oxygen is explained below:

$$m(CH_4) = 12 + 4(1) = 16$$

$$m(O_2) = 32$$

$$\text{Mass Ratio (Fuel/Air)} = m(CH_4)/m(O_2) = 16/32 = 0.5$$



$$\text{Stoichiometric (Fuel/Air) Mass ratio} = 1.(12 + 1.(4))/2.(16 \times 2) = 0.25$$

$$\text{Equivalence Ratio for Methane} = 0.5/0.25 = 2$$

Methane is a good example of a fuel to be used at low equivalence ratio.

In order for Plasma Combustion to be advantageous over pre heating transfer of energy between the electrodes has to occur at the chemical bend level. The energy in electron-neutral collision should not go in momentum transfer but should be so high that the ionization takes place forming a pool of radicals which will in turn accelerate the chemical reactions.

Plasma assisted combustion enhances the combustion performance at low equivalence ratio. In principle, plasma is generated by high voltage, nano second pulse duration and high repetitive rate pulses. The high reduced electric field during the pulse allows efficient electronic excitation and molecular dissociation, thereby generating a pool of chemically active radical species.

The energy exchange through the fast moving electron excites internal and external states moving the reagents away from thermal equilibrium. At low electron energy collision will result in large momentum transfer, Mid range collision and energy results in the excitation of vibrational modes. Ionization and dissociation of the molecules only occurs for collision energy above the ionization potential of the molecule. In order for plasma assisted combustion to be viable combustion enhancement technique, a significant portion of electrons should have energy above the ionization potential. In this section I evaluate the electron energy distribution function considering a realistic set of scattering cross sections.

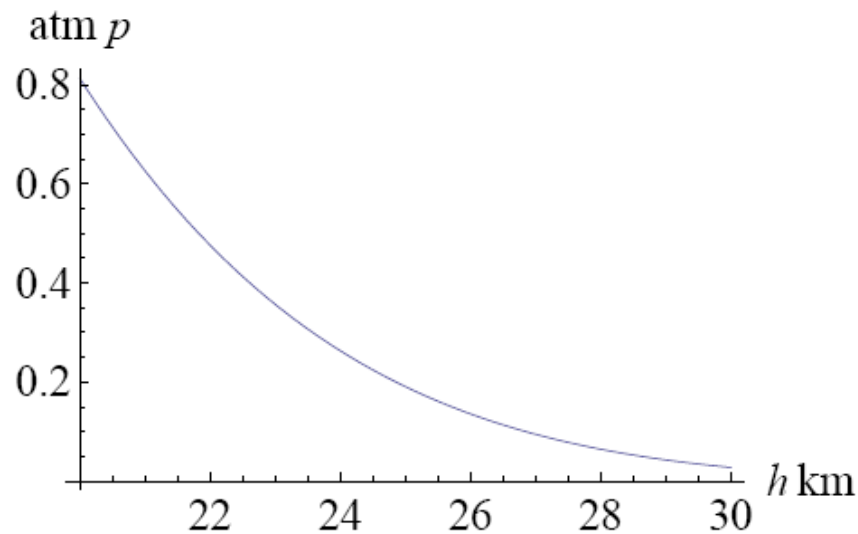


Fig 5.1: Pressure versus altitude for a  $M = 5$  flight and oblique entrance shocks providing the maximum allowable deflection. The ceiling altitude of 30 km was selected based on the target altitude of the NASA X43-A, initial design (data available at nasa.gov).

In light of the discussion above there is direct relationship between the reduced electric field and electron energy which makes the excitation process pressure dependent and hence in the case of hypersonic vehicle there is a strong dependency over the altitude.

In the application of High speed propulsion the  $E/N$  value can go upto 700 Td ( $1 \text{ Td} = 10^{-17} \text{ V cm}^2$ ) and using the multi term technique becomes a necessity. There is hardly any data available where the technique used in our research have been performed on Methane, especially at such conditions.

The necessary data needed for Methane which include cross sections and the energy domain of elastic and inelastic scattering collision processes, was taken from SHIRAI [2002][16].

The electron collision with methane resulting in elastic and inelastic scattering. The later includes the production of CH<sub>4</sub><sup>+</sup>, CH<sub>3</sub><sup>+</sup>, CH<sub>2</sub><sup>+</sup>, CH<sup>+</sup>, C<sup>+</sup>, H<sub>2</sub><sup>+</sup> and H<sup>+</sup> ion.

### 5.1 Analytic Expressions

The functional expressions used for the cross section of methane are those which are derived from semi empirically by Green and McNeal [17]. First we introduce three different functions in the form,

$$f_1(x; c_1, c_2) = \sigma_0 c_1 (x/E_R)^{c_2} \quad (i)$$

$$f_2(x; c_1, c_2, c_3, c_4) = f_1(x; c_1, c_2) / [1 + (x/c_3)^{c_2+c_4}] \quad (ii)$$

$$f_3(x; c_1, c_2, c_3, c_4, c_5, c_6) = f_1(x; c_1, c_2) / \left[ 1 + \left( \frac{x}{c_3} \right)^{c_2+c_4} + \left( \frac{x}{c_5} \right)^{c_2+c_6} \right] \quad (iii)$$

with  $\sigma_0 = 1 \times 10^{-16} \text{ cm}^2$  and  $E_R = 1.361 \times 10^{-2} \text{ keV}$  (Rydberg constant). Equation (i) to (iii) be general equations with the index  $x$  and  $c_i$  ( $i = 1, 2, 3, 4, 5, 6$ ) being dummy parameters.

The cross section for elastic collision process is of the following form:

$$\sigma = f_1(E_1; a_1, a_2) + f_2(E_1; a_1, a_2, a_3, a_4)$$

And the cross section for the inelastic collision process is of the following form:

$$\sigma = f_3(E_1; a_1, a_2, a_3, a_4, a_5, a_6)$$

Where,  $E_1 = E - E_{th}$  with  $E$  being the incident electron energy in KeV and  $E_{th}$  the threshold energy reaction in KeV.

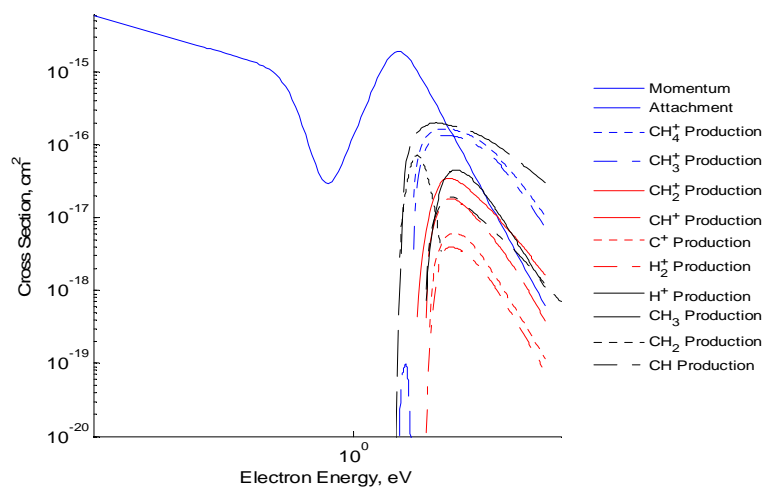


Fig 5.2: The cross section for methane breakdown into ions production with respect to electron energy.

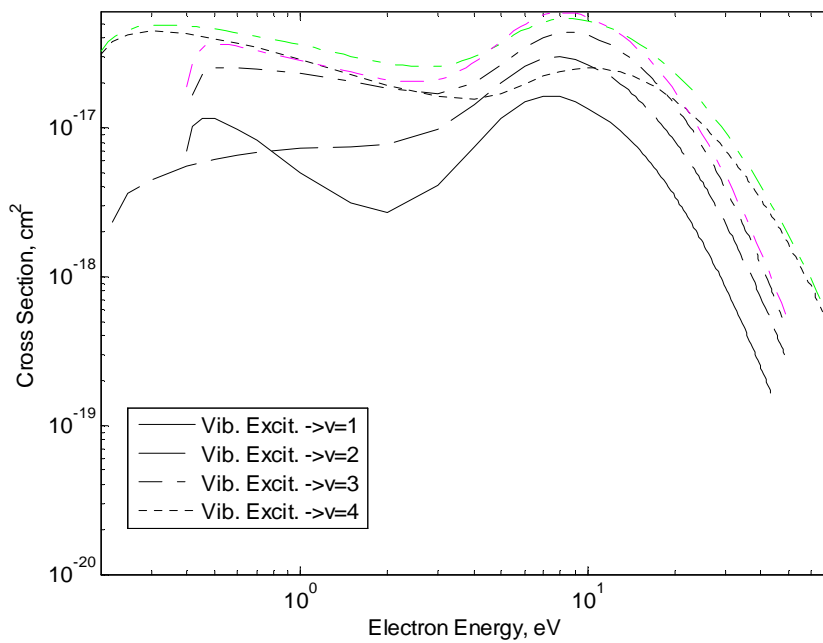


Fig 5.3: Methane's vibrational modes at low electron energy

Table 5.1 Energy range of data and parameter of the Analytic Expressions for Methane(CH<sub>4</sub>).

	1	2	3	4	5	6	7
a <sub>1</sub>	4.886	2.35	1.21-1	1.038	6.4-2	4.9-3	4.949-2
a <sub>2</sub>	1.627	1.435	1.868	1.161	1.43	3.61	2.855
a <sub>3</sub>	7.420-3	1.13-2	3.44-2	2	1.330-2	2.57-2	3.18-2
a <sub>4</sub>	-4.5-2	7.4-2	3-1	6.7-1	-3.3-1	-3.9-2	-3.3-1
a <sub>5</sub>	3.3-2	5.5-2	5.52-2	1.4-1	4.24-2	4.4-2	5.13-2
a <sub>6</sub>	1.04	1.2	1	1.6	1.181	1.29	1.155
E <sub>th</sub>	1.299-2	1.424-2	1.520-2	2.414-2	2.820-2	2.023-2	1.800-2

Explanation of Table

No.	Number label identifying a particular reaction process
$E_{th}$	Threshold energy of the reaction
$a_j$	Fit Parameters. The notation 1.23 – 1 means $1.23 \times 10^{-1}$ .

The pyrolysis of methane (conversion without addition oxygenated compound) in dielectric barrier discharge(DC) requires considerable consumption of energy. For the Methane degradation (eV/molecule) is 38eV and higher values.

For the different values of  $E/N$  we obtain the following results:

Table 5.2 Mean electron energy and drift velocity at 10 term and 2 term approximation.  $U_\infty=40$  eV.

$E/N$ (Td)	$u_m$ (eV)		$w$ ( $10^7$ cm s $^{-1}$ )	
	$L=10$	$L=2$	$L=10$	$L=2$
100	17.9611	18.6026	3.1909	3.1909
250	16.3328	18.5963	8.0546	8.0526
500	13.874	18.5799	16.1175	16.1144
700	12.6753	18.5666	22.5526	22.5493
800	12.2674	18.558	25.7661	25.2768
1000	11.6947	18.5464	32.1858	32.1825

Where,  $u_m = \int_0^\infty U^{\frac{3}{2}} f^{(0)}(U) du$

$$w = -\frac{1}{3} \left( \frac{2}{m_e} \right)^{\frac{1}{2}} \int_0^\infty U f^{(1)}(U) dU$$

We observe that the mean electron energy ( $u_m$ ) at multi term approximation goes down with the increase in reduced electric field whereas drift velocity increases with the same.

The distribution function at 40 eV and 100, 250, 500, 700 Td respectively is shown in fig 5.4:

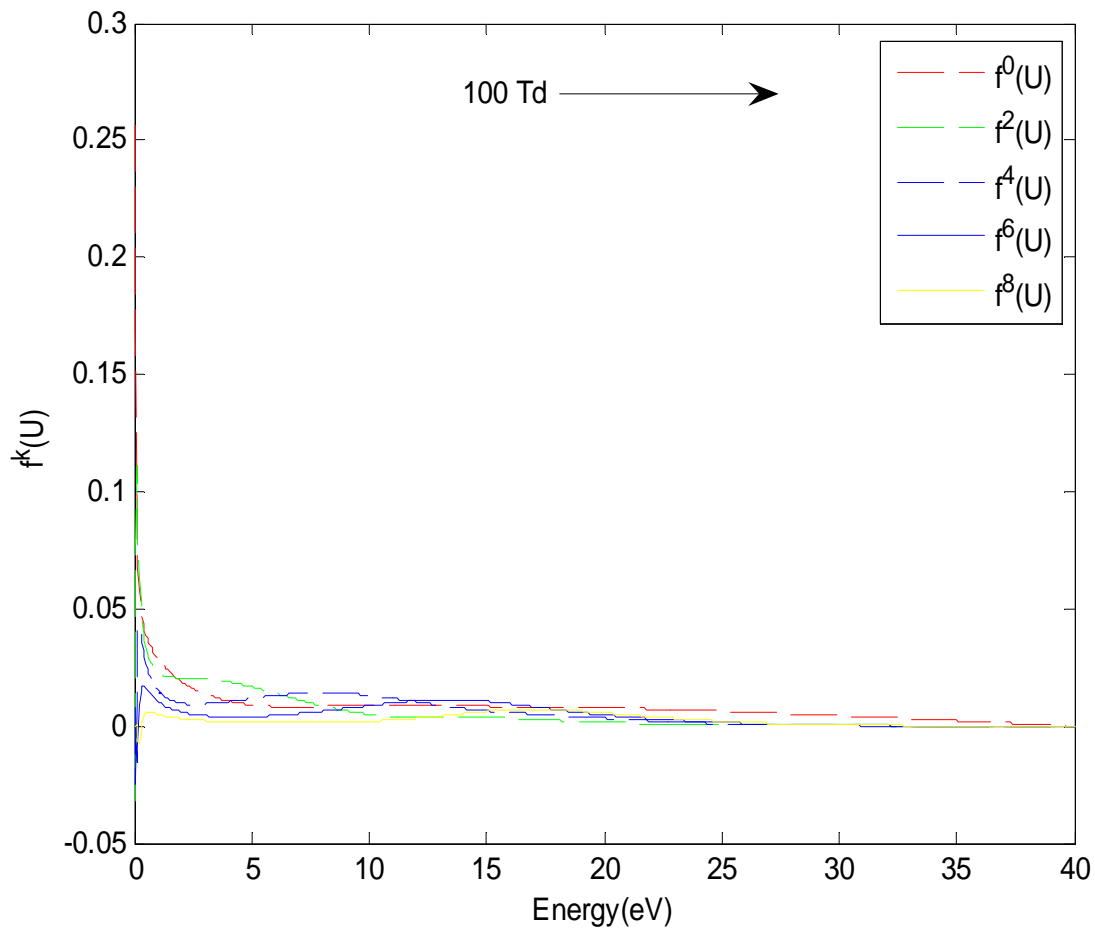


Fig 5.4: Distribution function At 40 eV, 100 Td and 100, 250,500,700 Td respectively.

We observe that all the function with lower and higher order expansions are very close to each other at this value of reduced electric field ( $=35.4 \text{ V cm}^{-1}\text{Torr}^{-1}$ ). As we raise the value of reduced electric field, higher and the lower order expansion begins to show the difference as shown in the figure 5.5 below:

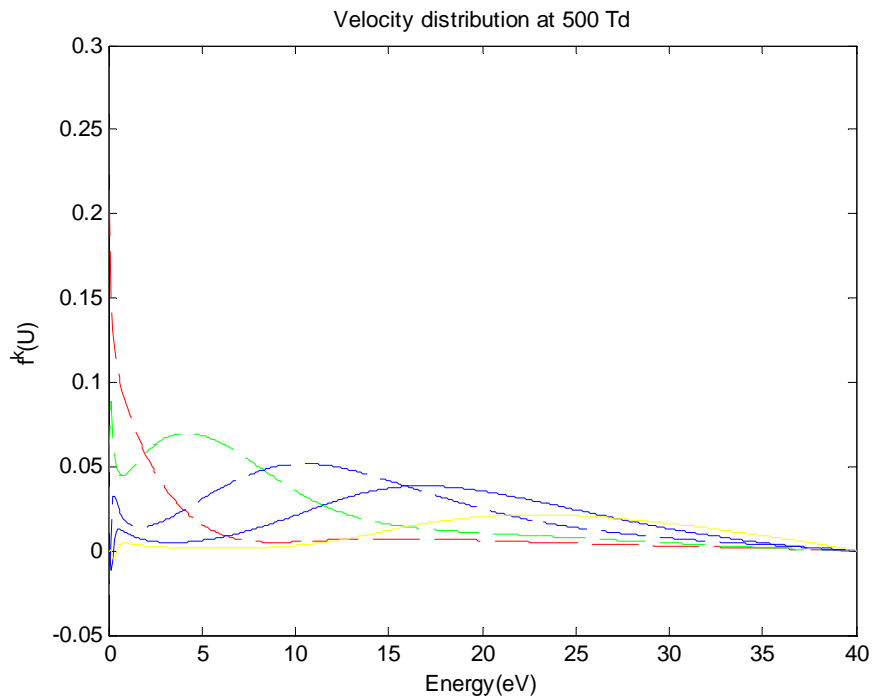
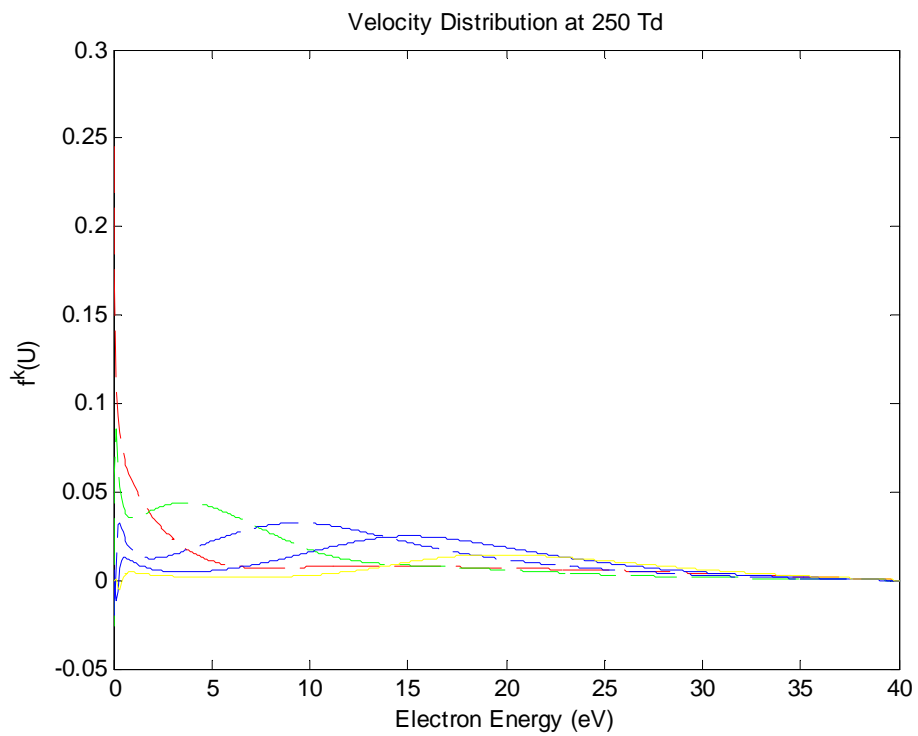


Fig 5.5: Energy distribution functions at 100 and 250 Td.

We can observe the large differences between higher and lower term expansion at a very low ambient pressure which is generally in case of Hypersonic flights occurring at a very high altitude. As expressed in Fig.

In fig 5.7, we observe the correction to the same expansion function at lower and higher term approximation of the Boltzmann equation.

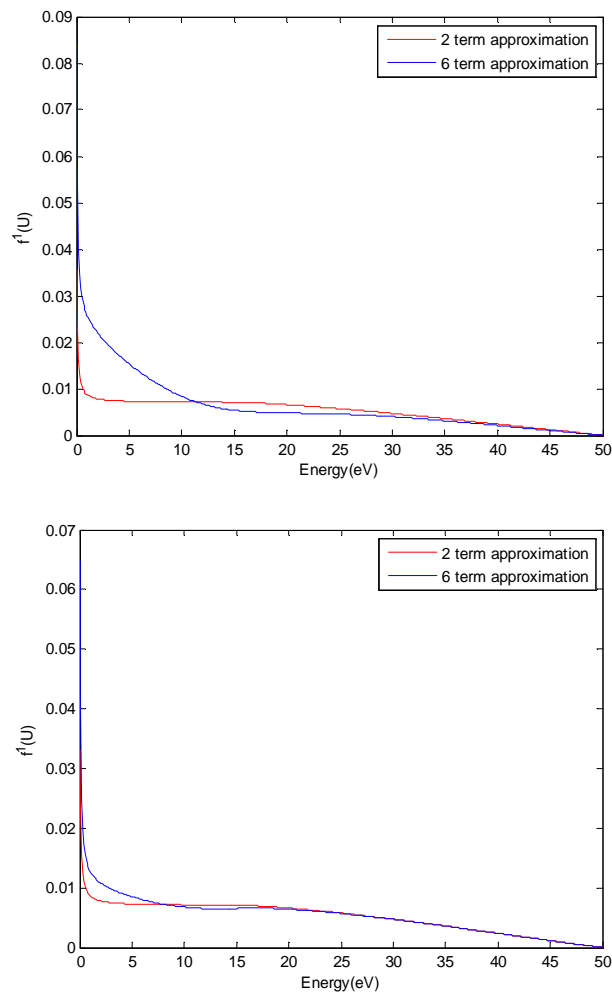


Fig 5.6: Comparison of 2 term and 6 term approximation at 50 eV for  $CH_4$  at 100 and 500 Td.

Keeping the electron energy constant to 50 eV the variation in the 1<sup>st</sup> term expansion term is observed at various E/N values, which is shown in the figure.

All the isotropic expansion function merges to one value near 14 eV and later the converges at 50 eV.

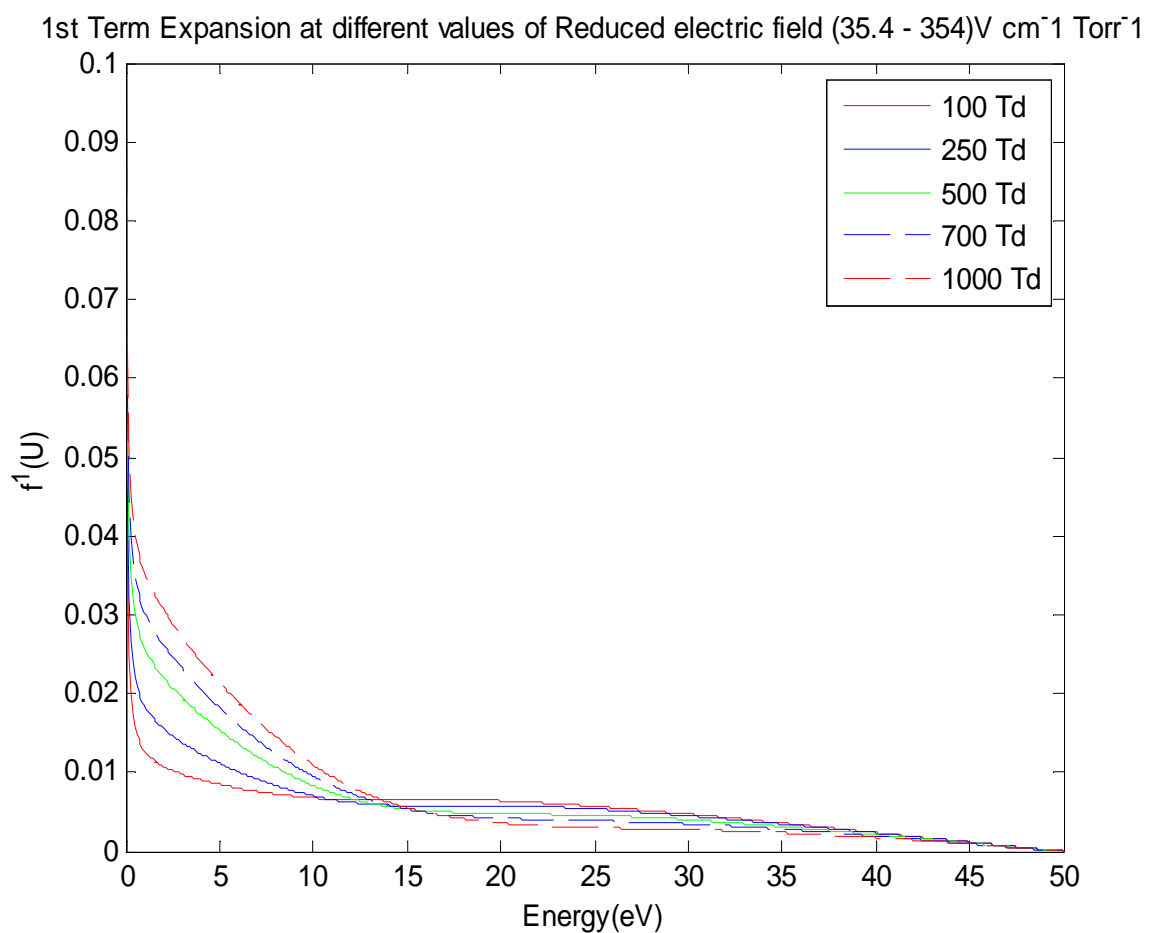


Fig 5.7: Isotropic function expansion(k=0) at various E/N values

## CHAPTER 6

### REACTION RATE COEFFICIENTS FOR METHANE

Our next step is to use the energy distribution function to define the reaction rate coefficient and as a future work, these rate coefficient will be used for the flame simulations and flame speed calculations.

We make use of the following general expression to express the rate coefficient relation with the distribution function:

$$k_k = \gamma \int_0^{\infty} U Q_{in,m}^{(0)} f^0(U) dU$$

Where,  $\gamma = (2e/m)^{1/2}$

Rate coefficients are calculated for every inelastic  $m^{th}$  process using 6 term approximation, and maximum electron energy of 50 eV. Results for every inelastic process are shown in figure 5.9.

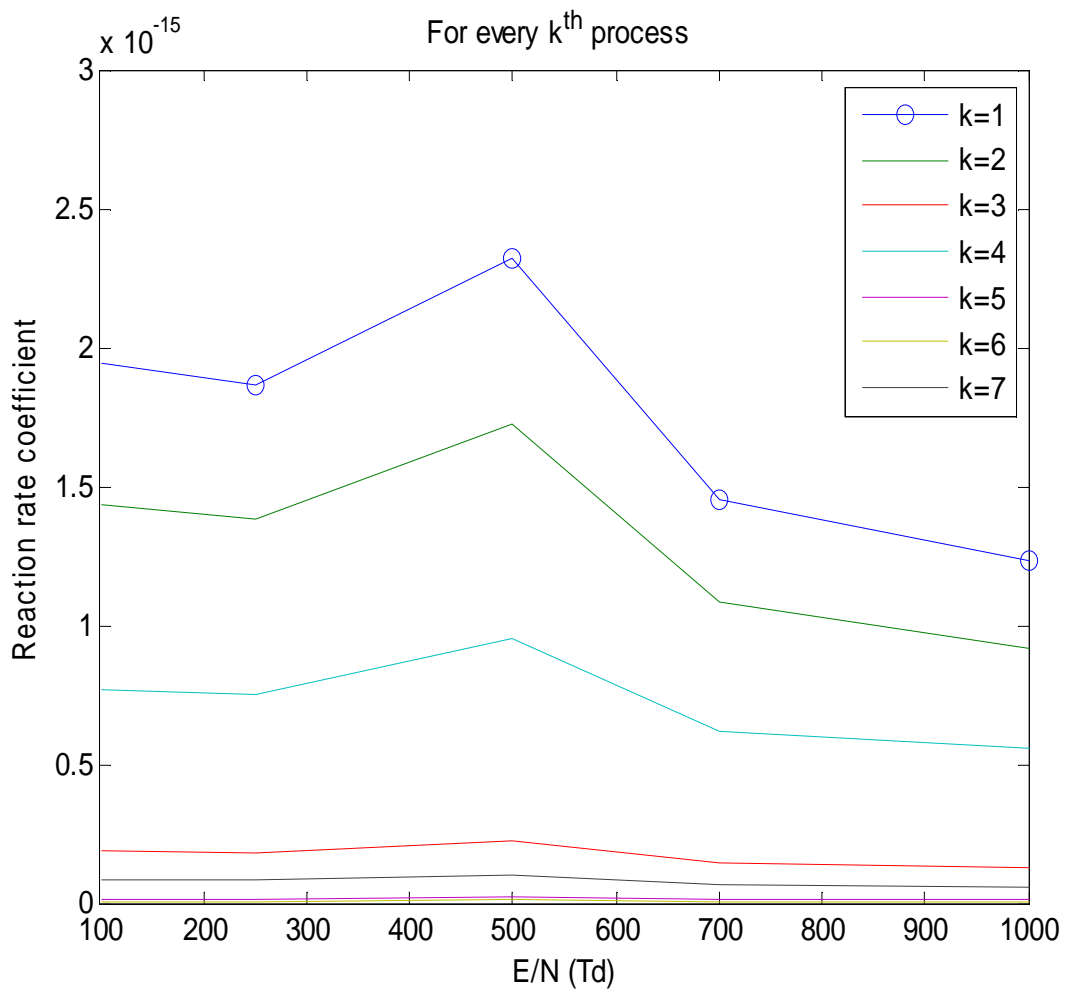


Fig 6.1: Reaction rate coefficient at different E/N interval

## CHAPTER 7

### CONCLUSIONS

A numerical algorithm for the solution of the Boltzmann equation in the steady-state limit was developed, validated and applied to the determination of the reaction rates for the production of methane ions. The objective of the research is to simulate conditions typical of plasma assisted combustion for aeronautical propulsion. Results achieved using the finite difference method are in agreement with the established results. The code developed in Matlab to perform finite difference analysis is computationally efficient when compared to literature algorithms thanks to the usage of a novel sparse matrix structure.

The validation test performed on the model gas gave excellent agreement with the referred results. The distribution curve with respect to the electron energy reaches its peak around 1 eV.

At high values of reduced electric field due to inconsistency of lower order expansion, multi term solution for the determination of Electron energy distribution function becomes a necessity.

The obtained distribution from the Boltzmann code is finally used to determine reaction rate coefficients for CH<sub>4</sub> for different values of reduced electric field ranging from 100 to 1000 Td.

APPENDIX A  
BOLTZMANN CODE

The Boltzmann code developed in MATLAB

```
function [U,f,w] = boltzmann
% indeendent variable
E_p0 = 17.7; %V cm^-1 Torr^-1
%system size
ninf = 1000;
ninfp1 = ninf+1;
L = 8;
Nall = ninfp1*L;
M = 1; %number of inelastic processes
e0 = 1; %measure energy in electron volt and fild in Volt
ng = 3.54d16; % cm^(-3)Torr^(-1)
%physical constants
me = 5.4857990943d-4; % amu
Ma = 4; %amu
Uinf = 15;
U = linspace(0,Uinf,ninfp1);
DU = mean(diff(U));
for m = 1:M
    Uin(m) = 1;
end
```

```

%inelastic processes

for m = 1:M
    nmv(m) = floor(Uin(m)/DU);
end

%system matrix
Mat = sparse(Nall,Nall);

%determine vectors
E_N = E_p0/ng;
me_M = me/Ma;

for i =1:ninfp1
    Qdv(i) = Qd(U(i));
    Qinsumv(i) = Qinsum(U(i) + DU/2);
    Qel0v(i) = Qel(0,U(i) + DU/2);
end

DQd = diff(Qdv)/DU;
kv = 1:(L-1);

for i =1:ninf;disp(i/ninf)
    Uiph = U(i) + DU/2; % ???????
    Qdph = Qd(Uiph);
    D(i) = -Uiph^2*me_M*Qdph;
    F(i) = -Uiph*2*me_M*(2*Qdph + Uiph *DQd(i) ) + Uiph * Qinsumv(i);
    for k = kv
        H(k,i) = Uiph*(Qel0v(i) - Qel(k,Uiph) + Qinsumv(i));
    end
end

```

```

ev(i) = -D(i)+F(i)*DU/2;
gv(i) = D(i) + F(i)*DU/2;
pm(kv,i) = H(kv,i)*DU/2;
rm(kv,i) = kv./(2*kv+1)*e0 *E_N.*(Uiph-(kv+1)*DU/4);
sm(kv,i) = -kv./(2*kv+1)*e0 *E_N.*(Uiph+(kv+1)*DU/4);
vm(kv+1,i) = kv./(2*kv-1)*e0 *E_N.*(Uiph+(kv-1)*DU/4);
wm(kv+1,i) = kv./(2*kv-1)*e0 *E_N.*(-Uiph+(kv-1)*DU/4);
end
%stack up the matrix
ieqn=0;
for i = 1:ninf
    ieqn = ieqn+1;
    indxs = [indx(1,i:i+1),indx(0,i:i+1)];
    Mat(ieqn,indxs) = [rm(1,i),sm(1,i),ev(i),gv(i)];
    for k = 1:L-2
        ieqn = ieqn+1;
        indxs = [indx(k+1,i:i+1),indx(k,i:i+1),indx(k-1,i:i+1)];
        Mat(ieqn,indxs) = [rm(k+1,i),sm(k+1,i),pm(k,i),pm(k,i),vm(k+1,i),wm(k+1,i)];
    end
    ieqn = ieqn+1;
    k=L-1;
    indxs = [indx(k,i:i+1),indx(k-1,i:i+1)];
    Mat(ieqn,indxs) = [pm(k,i),pm(k,i),vm(k+1,i),wm(k+1,i)];
end
end

```

```

neqn = ieqn;

%Add boundary conditions

ieqn= neqn; %determined in the large matrix loop

for k = 0:2:L-1

    ieqn=ieqn+1;

    Mat(ieqn,indx(k,ninfp1))=1;

end

for k = 1:2:L-1

    ieqn=ieqn+1;

    Mat(ieqn,indx(k,1))=1;

end

neqn=ieqn;

%Add right hand side, d matrix

ieqn = 0;

for i = 1:ninf

    for k =0:L-1

        ieqn = ieqn+1;

        for m = 1:M

            UiphpUi = U(i)+DU/2+Uin(m);

            DUlim = -DU*UiphpUi*Qin(k,UiphpUi,Uin(m));

            indxs = indx(k,i+nmv(m) +(0:2));

            rowl = DUlim*[1/2*alphan(-3,m)*alphan(-1,m),-alphan(1,m)*alphan(-
3,m),1/2*alphan(1,m)*alphan(-1,m)];

            ii = find(indxs <= Nall);

```

```

        Mat(ieqn,indx(ii)) = Mat(ieqn,indx(ii)) + rowl(ii);
    end
    Mat(ieqn,:) = Mat(ieqn,+)/E_N;
end
end
%normalization condition on the eigenvalue
%Modify the first equation
lambda = 2/4^(1/3);
tdur = sqrt((2*DU));
sqU = sqrt(U);
h = zeros(1,ninfp1);
h(1) = 2/3*tdur*(1 + 2*(lambda-1)*(lambda-2));
h(2) = -8/3*tdur*lambda*(lambda-2);
h(3) = 2/3*tdur*(1 + 2*(lambda-1)*lambda) + sqU(3);
for i = 2:(ninfp1)/2
    h(2*i) = 4*sqU(2*i);
    h(2*i+1) = 2*sqU(2*i+1);
end
h(ninfp1) = 4*sqU(ninfp1);
h(ninfp1) = sqU(ninfp1);
ieqn = 1;
indx = indx(0,1:ninfp1);
Mat(ieqn,indx) = h;
%right hand side of the equations

```

```

rhs = sparse(Nall,1);
rhs(1) = 3/DU;
f = full( reshape(Mat\rhs,L,ninfp1)');
%dimensional constants
wscal = sqrt(1.6021765314d-19/9.10938215d-31)*100 * 1d-7;
wint1 = U.^(3/2).*f(:,1).';
wint2 = U.*f(:,2).';
w(1) = quadl(@(x) interp1(U,wint1,x,'pchip'),min(U),max(U));
w(2) = -quadl(@(x) interp1(U,wint2,x,'pchip'),min(U),max(U))/3*sqrt(2)*wscal;
% w(1) = discrint(U,U.^(3/2).*f(:,1).');
% w(2) = -discrint(U,U.*f(:,2).')/3*sqrt(2)*wscal;

function out = indx(k,i)
    out = (i-1)*L + k +1;
end

function out = alpham(j,m)
    out = Uin(m)/DU-nmv(m)+j/2;
end

function out = Qd(Ui) %momentum transfer cross section
    out = Qel(0,Ui) - Qel(1,Ui);
end

function out = Qinsum(Ui)
out = 0;
    for mi = 1:M
        out = out + Qin(0,Ui,Uin(mi));
    end

```

end

end

end

## REFERENCES

- [1] Gregory. Safety Standard for Hydrogen and Hydrogen Systems. NSS 1740.16, NASA (1997).
- [2] Matveev and Rosocha. Guest editorial: special issue on plasma-assisted combustion. IEEE. Trans. Plasma Sci. 35:1605, (2007).
- [3] Starikovskaia. Plasma assisted ignition and combustion. J. Phys. D 39:R265-R299, (2006).
- [4] ONR Broad Agency Announcement Number 08-019.
- [5] Kim, Mungal and Cappelli. Formation and role of cool flames in plasma-assisted pre-mixed combustion. Appl. Phys. Lett. 92:051503, (2008).
- [6] Kim, Do, Mungal and Cappelli. Plasma-Discharge Stabilization of Jet Diffusion Flames. IEEE. Trans. Plasma Sci. 34:2545, (2006).
- [7] Nishimura and Gianturco. Vibrational excitations of CH<sub>4</sub> by electron impact: a close-coupling treatment. J. Phys. B 35:2873, (2002).
- [8]. H.Leyh, D. Loffhagen, R. Winkler, Computer Physics Communications 113 (1998) 33-48.
- [9] R. Winkler. G.L. Braglia, J. Wilhelm. II Nuovo Cimento D 10 (1988) 1209.
- [10] R. Winkler, G.L. Braglia. A. Hess. J. Wilhelm, Beitr. Plasmaphys. 24 (1984) 657.
- [11] D. Loflhagen, R. Winkler. J. Phys. D 29 (1996) 618.
- [12] G. Petrov, R. Winkler, J. Phys. D 30 (1997) 53.

- [13a] D.U. von Rosenherg, *Methods for the Numerical Solution of Partial Differential Equations* (American Elsevier. New York. 1961 ).
- [13b] D. Loflhagen, R. Winkler, *J. Comput. Phys.* 112 (1994) 91.
- [14] Schmidt, Wegmann, Huebner, and Boice. Cometary gas and plasma flow with detailed chemistry. *Comput. Phys. Commun.* 49:17, (1988).
- [15] Bao, Utkin, Keshav, Lou, and Adamovich. Ignition of Ethylene-Air and Methane-Air Flows by Low-Temperature Repetitively Pulsed Nanosecond Discharge Plasma. *IEEE. Trans. Plasma Sci.* 35:1628, (2007).
- [16] SHIRAI, *Atomic Data and Nuclear Data Tables* **80**, 147–204 (2002)
- [17] A. E. S. Green and R. J. McNeal, *J. Geophys. Res.* **76**, 133 (1971)
- [18] [ L.C. Pitchford. S.V. O'Neill. J.R. Rumble. *Phys. Rev. A* 23 ( 1981 ) 294.
- [19] R. Winkler. J. Wilhelm, A. Hess. *Beitr. Plasmaphys.* 23 (1983) 483.
- [20] P. Segur, M. Yousfi, M.C. Bordage. *J. Phys. D* 17 (1984) 2199.
- [21] K.F. Ness, R.E. Robson. *Phys. Rev. A* M (1986) 2185.

## BIOGRAPHICAL INFORMATION

Antriksh Luthra has received her Bachelor of Engineering degree in Mechanical Engineering from Visvesvariya Technological University, India, in July 2007. He is currently pursuing her Master's degree in Aerospace Engineering at The University of Texas at Arlington. He is a member of the honor engineering society, Tau Beta Pi and currently he is working in Plasma combustion project under Dr. Luca Massa, Aerospace Engineering, University of Texas at Arlington. His research interests include Plasma science and Plasma combustion.